АТОМНА ЕНЕРГЕТИКА
ATOMIC ENERGY

УДК 621.039.5 https://doi.org/10.15407/jnpae2023.03.231

O. M. Khotiaintseva[1,*], O. R. Trofymenko[1,2], V. M. Khotiaintsev[3], A. V. Nosovskyi[1,2], S. E. Sholomytsky[2], V. I. Gulik[1,2]

[1] *Institute for Safety Problems of Nuclear Power Plants, National Academy of Sciences of Ukraine, Kyiv, Ukraine*
[2] *Limited Liability Company ENERGORISK, Kyiv, Ukraine*
[3] *Taras Shevchenko National University of Kyiv, Kyiv, Ukraine*

*Corresponding author: olenakhot@gmail.com

CALCULATION OF RADIATION FIELDS IN THE VVER-1000 CONCRETE BIOLOGICAL SHIELD USING MONTE CARLO CODE SERPENT[a]

To calculate radiation fields in the concrete biological shield (CBS) of the VVER-1000 reactor in this work, we have developed and applied the Monte Carlo code Serpent simulation framework based on the variance reduction technique. We have quantified the radial, axial, and azimuthal variation of neutron and gamma-ray fluxes and the absorbed dose rate in the CBS. Using the calculation results, we estimate maximum neutron fluence and maximum absorbed dose in the VVER-1000 CBS over the period of 60 and 80 years of the reactor operation and localize the domains of highest radiation exposure. The obtained results are in good agreement with the available data on the VVER-1000 and other pressurized water reactors. We show that the fluence of neutrons with energy above 0.1 MeV decreases by half at a depth of 4 cm of concrete, and the gamma-ray absorbed dose decreases by 40 % at a depth of 13.5 cm. The outcomes from this research will help to assess the effects of prolonged irradiation of the VVER-1000 CBS, which is required for reliable risk assessment for extended operation of nuclear power plants.

Keywords: concrete biological shield, irradiated concrete, Monte Carlo code Serpent, VVER-1000.

1. Introduction

The aging of nuclear power plants (NPPs) in many countries raises a problem of the lifetime extension of NPPs. Concrete structures of nuclear reactors provide both strength and a biological shield. So, it is important to assess the effect of radiation exposure on the concrete biological shield (CBS) and other concrete structures of nuclear reactors. This requires the assessment of the radiation environment in the concrete structures, experimental studies on irradiation of concrete samples, and experimental and theoretical studies in material science. The paper [1] reviews the results of experimental and theoretical studies on irradiated concrete and outlines the tasks to be solved to extend the lifetime of NPPs for 60, 80, and more years. Since the radiation environment varies with the reactor type, design, and composition, assessing the radiation environment for each specific reactor is an important task [1, 2]. The radiation exposure should be assessed for a certain reactor operation time. The criteria used to assess whether the mechanical properties of the irradiated concrete change, follow from the results of experiments on irradiation of concrete samples either by neutrons or gamma-rays. According to [3], "The structural capacity of the CBS will be affected by the depth of concrete where the neutron fluence exceeds the damage threshold of $1.0 \cdot 10^{19}$ n/cm^2 ($E > 0.1$ MeV) and/or the depth of the concrete where the gamma dose exceeds the threshold of $2.3 \cdot 10^{10}$ Rad". However, the experimental data presented in Fig. 2 of the work [1] shows that the mechanical properties of concrete deteriorate only by 15 % at a fluence of 4.0 10^{19} cm^{-2} while the data for different types of concrete scatter more than 30 %.

This work aims to simulate neutron and gamma-radiation fields in the reactor VVER-1000 with a specific focus on its CBS using the Monte Carlo code Serpent, and to develop a methodology that provides sufficient accuracy of the calculated spatial distributions of energy deposition and the radiation fluxes in the CBS. The final aim is to estimate the maximum fluence and absorbed gamma-ray dose for 60 and 80 years of the reactor operation and to determine the concrete domains with the highest radiation exposure.

[a] Presented at the XXIX Annual Scientific Conference of the Institute for Nuclear Research of the National Academy of Sciences of Ukraine, Kyiv, September 26 - 30, 2022.

2. Neutron and photon transport simulation

In this work, we applied the Serpent code with the appropriate Evaluated Nuclear Data File cross-section libraries [4]. Earlier developed 2D and 3D Serpent models of the VVER-1000 [5, 6] were further improved and extended to include the reactor pressure vessel (RPV) and the CBS. Calculations were performed for the first fuel loading of the VVER-1000 at the Temelin NPP (Czech Republic) [7]. The detailed dimensions and material composition within the reactor barrel correspond to the benchmark [7]. The basic design parameters of the VVER-1000 are presented in Table 1.

Structural elements of the VVER-1000 reactor are shown in Fig. 1, *a* and *b*.

Table 1. **Some design parameters of the VVER-1000**

Thermal power	RPV inner radius	RPV outer radius	CBS inner radius	CBS outer radius
3000 MW	206.80 cm	226.75 cm	290.50 cm	363.50 cm

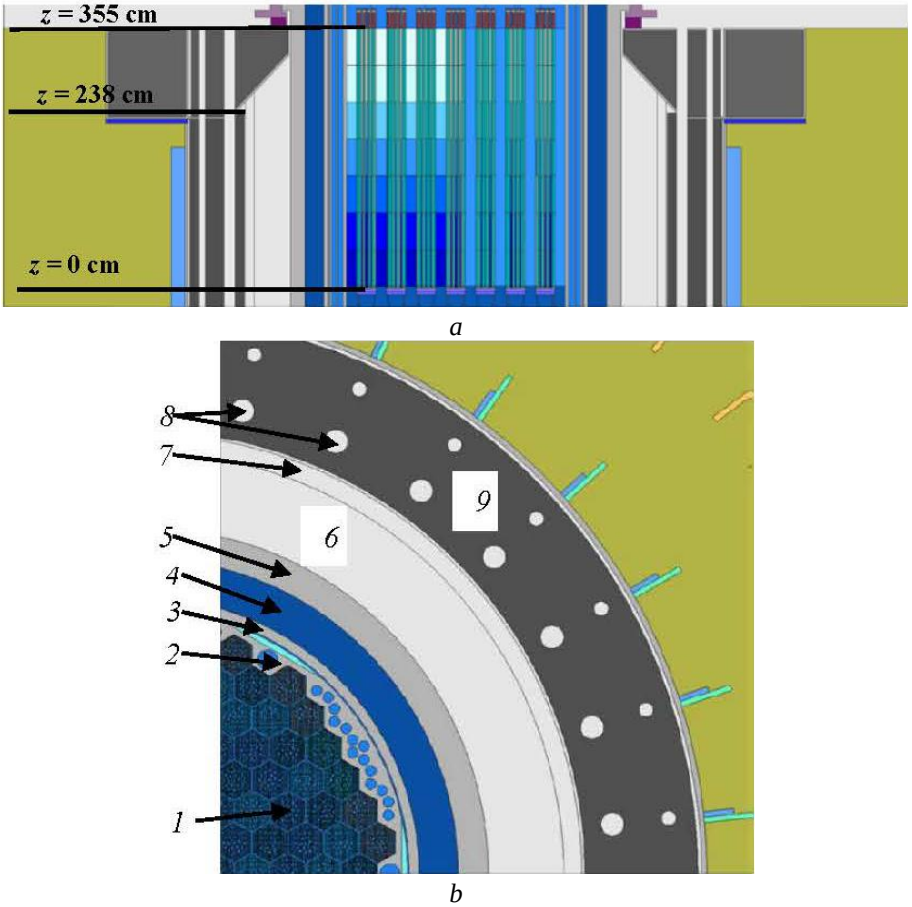

Fig. 1. The 3D model of the VVER-1000 in the Serpent code. *a* – axial cross-section: z = 355 cm is the top of the fuel, z = 238 cm is the top of the CBS, z = 0 is the bottom of the fuel; *b* – a fragment of the radial cross-section: *1* – reactor core, *2* – baffle, *3* – barrel, *4* – coolant, *5* – RPV, *6* – air cavity, *7* – thermal isolation shield (replaced by air in the present study), *8* – ionization chamber channels, *9* – CBS. (See color Figure on the journal website.)

The Serpent code is a modern Monte Carlo tool for various reactor calculations, including the generation and transport of neutrons and gamma-rays [4, 8]. The task of the presented simulation is to calculate with appropriate accuracy the radial, angular, axial, and spectral distributions of neutron and gamma-radiation in the CBS. In an operating reactor, neutrons and gamma-rays are generated mainly in the reactor core. Several layers of metal and water between the core and the CBS attenuate neutron and photon fluxes by five orders of magnitude and more. So, only a small fraction of all generated neutrons and gamma-rays reach the CBS. Because of that, direct Monte Carlo calculation of the radiation fields in the CBS with appropriate accuracy requires playing out a large number of initial histories, and the computer run-time, which is roughly proportional to the number of histories, becomes unrealistically long. This provides the main challenge for the calculations presented in this work. To achieve the appropriate accuracy, we applied the variance reduction technique recently implemented in the Serpent code [9].

Serpent provides two methods for neutron transport calculations: *criticality source simulation*

and *external source simulation*. In the criticality source simulation, both neutron source and neutron transport are calculated together, iteratively. In the external source simulation, neutron transport is calculated for a given user-specified source. Both methods allow an option for coupled neutron-photon calculation [8]. Serpent provides also a method for separate photon transport calculation from a user-specified source. Sources of neutrons and photons can be written into files during the criticality calculation (the photon source can be written in the coupled neutron-photon calculation mode).

In Serpent, the variance reduction technique can be applied to transport calculations only in the external source simulation [9]. Therefore, to apply the variance reduction, it is necessary first to perform a criticality source simulation and write the source into a file, and then to calculate transport with the external source using the file written in the previous calculation.

In addition to neutron reactions, photons result also from the radioactive decay of fission products and transuranic isotopes that are produced in the core during the reactor operation. To calculate the transport of photons from radioactive decay, we need to know the isotopic composition of the reactor after some period of its operation. For this purpose, Serpent provides a *depletion calculation* mode which is a burnup calculation with writing material compositions into a restart file at each burnup step.

Having tested different combinations of the available calculations in Serpent, we have chosen and applied in this work the following calculation scheme.

1. Criticality source simulation, writing neutron source into a file.

2. Coupled neutron-photon transport calculation with the pre-written external neutron source, using variance reduction technique.

3. Step-by-step depletion calculation, writing the core isotopic composition into a restart file at each burnup step.

4. Transport calculation of photons from radioactive decay using radioactive decay source mode, and variance reduction technique.

Changes in the core material composition with burnup affect the production and transport of neutrons and gamma-rays from neutron reactions. To assess the effect of these changes, we performed criticality source simulations for the material composition at several burnup steps, writing neutron source into a file, and then performed coupled neutron-photon transport calculation with the pre-written external neutron source, applying variance reduction technique. In the burnup calculations and criticality source calculations at different burnups, we used the boron concentration matching option to keep k_{eff} equal to 1, maintaining in such a way a realistic neutron balance and the ratio between fissions and captures in the core.

Our choice of the presented calculation scheme was based on the results of the trial calculations. A low number of histories in criticality source simulation leads to poor quality of the particle source and low accuracy in a subsequent transport calculation with such a source; a higher number of histories increases the run-time and the size of the particle source file. For the neutrons, accuracy becomes acceptable at reasonable run-time and source file size, while for the photons the situation is different. Neutrons are produced only in the reactor core, but photons from neutron capture are produced everywhere in the reactor. Photons from neutron capture in the CBS give a significant share of total photon flux in the CBS. Since very few of all neutrons reach the CBS, sufficient quality of a photon source requires too high initial statistics at an unrealistic source file size. So, we refused to write and use the photon source; instead, we wrote the neutron source with sufficient initial statistics, and calculated photon transport in a coupled neutron-photon transport calculation requiring only the neutron source. To avoid neutron multiplication, we excluded neutron generation in fission reactions using the corresponding Serpent option, while the photon emission in fission was preserved.

In this work, we used mainly global variance reduction with cylindrical weight window mesh which uniformly populated the entire geometry. To determine neutron flux in the ionization chamber channels of the CBS, we applied variance reduction for a single detector. Fig. 2 illustrates the effect of global variance reduction on the statistical error of the azimuthal distribution of neutron flux.

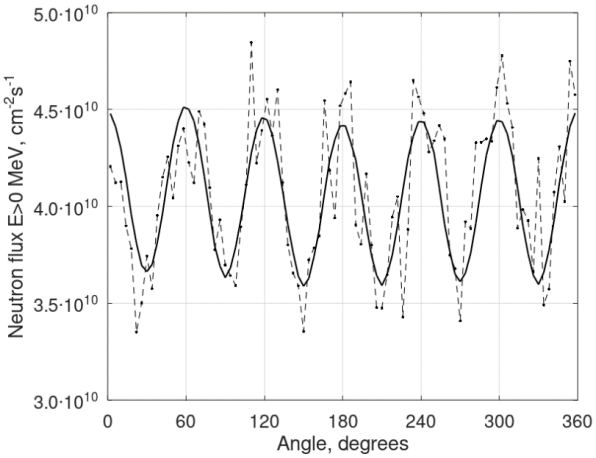

Fig. 2. Azimuthal distribution of the total neutron flux $(E > 0)$ in the inner surface layer (1 cm thick) of the CBS, Serpent calculations with (solid line) and without (dashed line) variance reduction.

The dashed line represents the result of the criticality calculation at $2 \cdot 10^9$ initial histories and 40 h of run-time. The solid line represents the result of applying the global variance reduction at 10^8 initial histories and three iterations and about 30 h of the run-time.

Fig. 2 shows that in spite of high statistics and run-time, the criticality calculation fails to resolve the angular dependence well, even near the inner surface of the CBS where the flux is greatest. At the same time, variance reduction improves statistical error dramatically, and the calculation in three iterations yields a practically ideal fluent curve. On the other side, a clear agreement between the results of independent calculations shown in Fig. 2 confirms that variance reduction does not distort the results.

Using the appropriate flux and energy deposition tallies in the Serpent code, we obtained neutron fluxes with different energy cutoffs, photon fluxes, dose rates, and their radial, angular, and height distributions in the CBS. In this study, we use Serpent version 2.1.32 and data libraries with KERMA coefficients (Kinetic Energy Release in MAterials) based on ENDF/B-VII.1 [10].

3. Results and discussion

We estimated the values of interest in the CBS by means of special tallies implemented in Serpent, the so-called detectors. To obtain flux distributions, we use a cylindrical mesh detector and detector energy binning. The Serpent code has several modes of energy deposition calculation [10]. We used the most accurate mode with the appropriate Serpent energy deposition detector, which provides both the total energy deposition and the energy deposition from neutrons and photons separately. Moreover, the energy deposited by all photons is accounted for at the site of deposition, not at the site of photon generation. This is especially important for secondary photons emitted in neutron captures in the CBS. The absorbed dose rate in Rad/s was calculated by the formula:

$$\dot{D} = 100 \frac{\dot{E}}{\rho V}, \qquad (1)$$

where $\dot{E}$ – the detector output, W cm^3 in the Serpent code; ρ – the concrete density, kg/cm^3; V – the detector volume, cm^3.

Fig. 3 shows height distributions of the azimuthally averaged neutron flux with two energy cutoffs calculated in the 1 cm thick near-surface layer of the CBS. The upper margin of 238 cm of the height distance in Fig. 3 corresponds to the top of the inner surface of CBS (above it, the concrete truss is located). Peak flux values (which are $4.05 \cdot 10^{10}$ cm^{-2}s^{-1} for the total flux and $1.29 \cdot 10^{10}$ cm^{-2}s^{-1} for the fast flux) are achieved at the height position corresponding to the middle of the fuel.

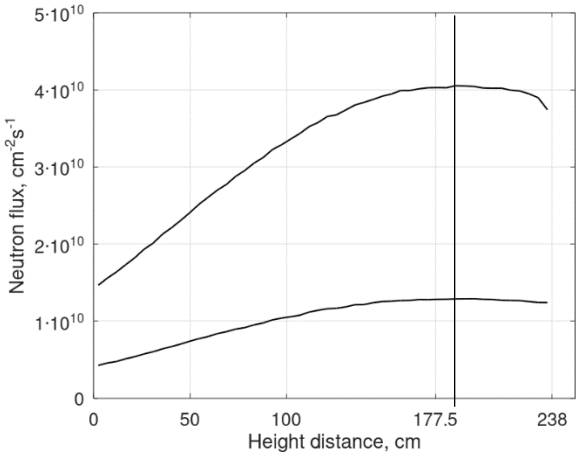

Fig. 3. Axial neutron flux distribution in a thin inner surface layer of the CBS in its central part in height relative to the fuel; *1* – total neutron flux ($E > 0$ MeV), *2* – fast neutron flux ($E > 0.1$ MeV). A vertical straight line denotes the height position corresponding to the middle of the fuel.

Table 2 shows the azimuthally averaged fluxes of neutrons and gamma-rays at the inner surfaces of the CBS and the concrete truss. The fact that the concrete truss is exposed to lower fluxes than the CBS is related to the location of the truss in the upper part relative to the fuel (see Fig. 1, *a*).

Table 2. **Neutron and gamma-ray fluxes at different height positions, at the inner surface of the concrete of the CBS and the truss**

Fluxes, cm^{-2}s^{-1}	z = 177.5 cm (CBS)	z = 272 cm (truss)	z = 321.5 cm (truss)
Total neutron flux $E > 0$	$4.078 \cdot 10^{10}$	$2.974 \cdot 10^{10}$	$2.718 \cdot 10^{10}$
Thermal neutron flux $E < 0.41$ eV	$7.154 \cdot 10^{9}$	$4.650 \cdot 10^{9}$	$2.555 \cdot 10^{9}$
Fast neutron flux $E > 0.1$ MeV	$1.368 \cdot 10^{10}$	$9.752 \cdot 10^{9}$	$8.911 \cdot 10^{9}$
Fast neutron flux $E > 1$ MeV	$1.487 \cdot 10^{9}$	$9.096 \cdot 10^{8}$	$7.772 \cdot 10^{8}$
Gamma-ray flux	$1.892 \cdot 10^{10}$	$1.148 \cdot 10^{10}$	$1.016 \cdot 10^{10}$

Fig. 4 shows the azimuthal distribution of fast neutron flux ($E > 0.1$ MeV) in the inner surface layer (1 cm thick) of the CBS in its central part in height relative to the fuel (averaged over 50 cm in height).

The maximum to minimum flux ratio is 1.4, average flux is $1.29 \cdot 10^{10}$ $cm^{-2}s^{-1}$. Almost periodic azimuthal dependence with a 60-degree period is related to the periodic geometry of the core.

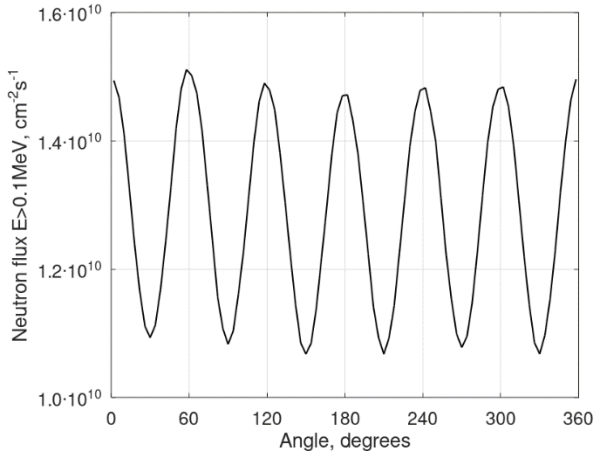

Fig. 4. Angular distribution of the fast neutron flux ($E > 0.1$ MeV) in the inner surface layer (1 cm thick) of the CBS.

Table 3 shows the ratio of maximum fluxes and dose rate to corresponding average values due to angular dependence.

Table 3. **The ratio of maximum values to average values in the first 1 cm layer of the CBS**

Flux and dose rate	Maximum value/ Average value
Total neutron flux E > 0	1.11
Thermal neutron flux E < 0.41 eV	1.06
Fast neutron flux E > 0.1 MeV	1.17
Fast neutron flux E > 1 MeV	1.23
Photon flux	1.24
Dose rate	1.29

Figs. 5 and 6 show radial dependencies of neutron and gamma-ray fluxes (Fig. 5), and dose rate (Fig. 6) in the first 15 cm of the CBS from the inner surface, in the central part in height relative to the fuel. The 15 cm thick layer of concrete 50 cm in height was divided into 20 equal radial bins, and average values over each bin were calculated.

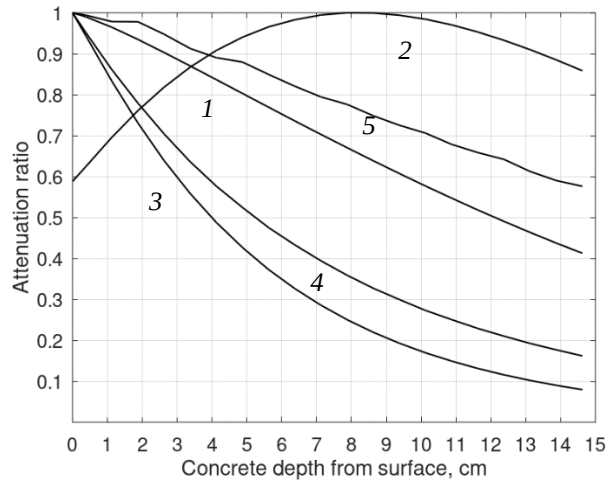

Fig. 5. Normalized radial distributions of particle fluxes in the first 15 cm of the CBS. *1* – total neutron flux $E > 0$; *2* – thermal neutron flux $E < 0.41$ eV; *3* – fast neutron flux $E > 0.1$ MeV; *4* – fast neutron flux $E > 1$ MeV; *5* – photon flux.

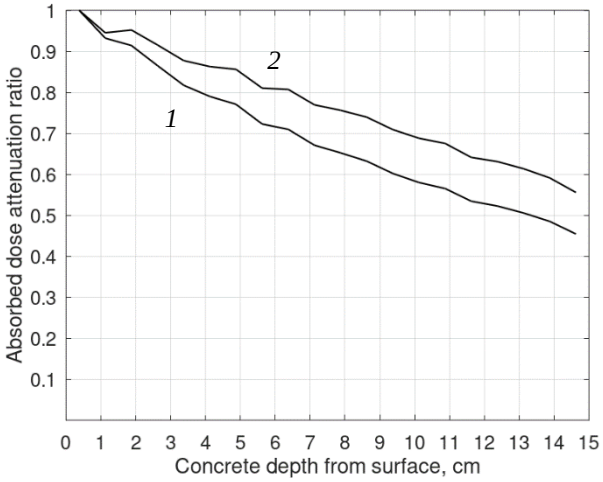

Fig. 6. Normalized radial distribution of the absorbed dose rates in the first 15 cm of the CBS in depth; *1* – total absorbed dose rate; *2* – gamma-ray absorbed dose rate.

The distributions shown in Figs. 5 and 6 are normalized to the corresponding maximum values of the CBS presented in Table 4. In Fig. 6, starting point of curves *1* and *2* corresponds to the center of the 0.75 cm thick first bin in the radial direction, in the concrete. A similar additional bin in the air directly near the inner CBS surface was used to estimate neutron and gamma-ray fluxes at the inner surface of the CBS.

Table 4. **Radiation fluxes and absorbed dose rates at the inner surface of the CBS**

Neutron fluxes, $cm^{-2}s^{-1}$				Gamma-ray flux, $cm^{-2}s^{-1}$	Absorbed dose rate, Rad/s	
$E > 0$	$E < 0.41$ eV	$E > 0.1$ MeV	$E > 1$ MeV		Total	Gamma-ray
$4.078 \cdot 10^{10}$	$7.154 \cdot 10^{9}$	$1.368 \cdot 10^{10}$	$1.487 \cdot 10^{9}$	$1.89 \cdot 10^{10}$	11.2	8.7

What concerns gamma-rays produced in radioactive decays, our calculation (according to items 3 and 4 of the calculation scheme described in Section 2) yields the flux of $7.8 \cdot 10^{7}$ $cm^{-2}s^{-1}$ on the inner surface of the CBS, which is only 0.4 % of the gamma-ray flux presented in Table 4 (which is a gamma-ray flux

from neutron reactions). So, the contribution of gamma-rays from radioactive decay can be neglected. In addition, our calculations have shown that changes with burnup in the core material composition affect neutron and gamma-ray fluxes and absorbed dose in the CBS less than 10 %.

As can be seen from Figs. 5 and 6, the flux of fast neutrons with the energies $E > 0.1$ MeV falls by a factor of 10 at the depth of 13 cm, and at the same depth, the gamma-ray dose rate falls only by nearly 40 %. In Fig. 5 all the presented neutron fluxes demonstrate different variations with the distance from the inner surface of the concrete. Due to the moderation and absorption of neutrons, both fast neutron fluxes (curves *3* and *4*) fall quickly with the distance from the inner surface. Since the high-energy neutron flux $E > 1.0$ MeV (curve *4*) falls slower than the flux $E > 0.1$ MeV (curve *3*), the share of the high-energy neutrons ($E > 1.0$ MeV) increases in the fast neutron flux $E > 0.1$ MeV. At the same time, thermal neutron flux grows in the first 8 cm of concrete, due to intense moderation of faster neutrons, and in spite of the absorption. Along with this, the total neutron flux (Fig. 5, curve *1*) falls almost linearly in the whole 15 cm layer of the CBS, and so do the total gamma-ray flux (Fig. 5, curve *5*), the total absorbed dose rate (Fig. 6, curve *1*), and the gamma-ray absorbed dose rate (Fig. 6, curve *2*). This testifies to the important contribution of secondary photons from radiative captures in the CBS, since the attenuation of photons coming from the core is near-exponential [11]. Relative statistical error of the presented results for neutron flux distributions was less than 0.5 %, while for the gamma-ray flux and dose rate distributions it was less than 2 %.

For the CBS of the reactor VVER-1000, the experimental data have been reported on the neutron flux in the ionization chamber channels of the CBS [12]. Using the activation method, the authors have obtained the value of $(1.08 \pm 0.2) \cdot 10^8$ cm^{-2}s^{-1} for the flux of neutrons $E > 1.2$ MeV in the center of the channel located at the azimuthal position 15 degrees, in the central part in height relative to the fuel. We calculated the same flux averaged over a 50 cm long part of a channel of a similar location, with a relative statistical error of 0.005. The calculated flux $1.30 \cdot 10^8$ cm^{-2}s^{-1} is in good agreement with the experimental value, taking into account possible differences in the fuel load.

Using the calculation data presented in Tables 3 and 4, we estimated the maximum neutron fluences with different energy cutoffs and absorbed doses at the inner surface of the CBS accumulated during 60 and 80 years of the reactor operation, assuming an 80 % capacity factor.

Table 5. **Predicted maximum neutron fluence and absorbed dose in the CBS accumulated over 60 and 80 years of operation, for the VVER-1000, 2-loop PWR, and 3-loop PWR**

Fluence and absorbed dose	60 years of operation			80 years of operation		
	VVER-1000	2-loop PWR	3-loop PWR	VVER-1000	2-loop PWR	3-loop PWR
Total neutron fluence $E > 0$, cm^{-2}	$6.9 \cdot 10^{19}$	$1.1 \cdot 10^{20}$	$5.4 \cdot 10^{19}$	$9.2 \cdot 10^{19}$	$1.5 \cdot 10^{20}$	$7.2 \cdot 10^{19}$
Fast neutron fluence $E > 0.1$ MeV, cm^{-2}	$2.4 \cdot 10^{19}$	$4.2 \cdot 10^{19}$	$2.0 \cdot 10^{19}$	$3.2 \cdot 10^{19}$	$5.6 \cdot 10^{19}$	$2.7 \cdot 10^{19}$
Fast neutron fluence $E > 1.0$ MeV, cm^{-2}	$2.8 \cdot 10^{18}$	$4.9 \cdot 10^{18}$	$1.3 \cdot 10^{18}$	$3.7 \cdot 10^{18}$	$6.5 \cdot 10^{18}$	$1.7 \cdot 10^{18}$
Total absorbed dose, Rad	$2.2 \cdot 10^{10}$	–	–	$2.9 \cdot 10^{10}$	–	–
Gamma-ray absorbed dose, Rad	$1.7 \cdot 10^{10}$	–	–	$2.3 \cdot 10^{10}$	–	–

Table 5 shows a reasonable agreement between the values predicted in this work for the VVER-1000, and similar available data for 2-loop and 3-loop pressurized water reactors (PWRs) [2].

4. Conclusions

This work is devoted to 3D calculations of radiation fields in the CBS of the VVER-1000 power nuclear reactor using the Serpent Monte Carlo code. On the way from the core to the biological shield, neutron and gamma-ray fluxes are greatly attenuated. In order to obtain reliable results with sufficient accuracy within a realistic computer run-time, we have developed a calculation scheme using the variance reduction technique, paying special attention to self-checking and consistency of the results.

From the obtained results, we have determined the maximum fluence of fast neutrons, the maximum absorbed dose, and the localization of domains of the CBS with the highest radiation exposure; these are the characteristics that determine the deterioration degree

of the mechanical properties of concrete and the stability of concrete structures during the long-term operation of VVER-1000. According to [1 - 3], no universally applicable threshold of radiation exposure exists: the deterioration of mechanical properties can be expected at fluences exceeding 10^{19} cm^{-2} and the gamma-ray absorbed dose exceeding $2.3\cdot10^{10}$ Rad, and the actual threshold depends on the cement brand, the technology of pouring of concrete during the construction, the type of reactor and its operating conditions. In each such case, additional detailed experimental studies of the radiation resistance of a specific type of concrete are recommended. If we take 10^{19} cm^{-2} for the fast neutron fluence ($E > 0.1$ MeV) and $2.3\cdot10^{10}$ Rad for the gamma-ray absorbed dose as the reference values, the following conclusions follow from the obtained results.

In the central part in height relative to the fuel of the near-surface layer of the CBS, the fast neutron fluence ($E > 0.1$ MeV) exceeds the reference value of 10^{19} cm^{-2} already in 21.4 years of reactor operation in some azimuthal positions, and in all azimuthal positions – in 29.3 years. During the 80-year operation period, the excess in fast neutron fluence is achieved in a layer of concrete up to 6.5 cm thick, in the most unfavorable height and azimuthal positions; the gamma-ray absorbed dose does not achieve the reference value of $2.3\cdot10^{10}$ Rad during the 80-year operation period. In the support truss, the achieved fast neutron fluence is lower, due to the location of the truss in the upper part relative to the fuel.

The estimates of fluence and dose obtained in this work for a long period of operation of the VVER-1000 reactor can help – together with the experimental studies of radiation damage of concrete and complex material science studies – to assess the risks of long-term irradiation of the CBS and the possibility of the life-time extension of the reactor VVER-1000.

The Serpent calculation scheme developed in this work can be applied (directly or with certain modifications) to estimate the radiation exposure to the CBS for each specific VVER-1000 unit and for VVER-440 reactors. In addition, the proposed calculation scheme can be useful for choosing the best material composition of the CBS of future reactors, including small modular reactors, which could be built in Ukraine.

The presented research was carried out within the framework of the Horizon 2020 project ACES. This project has received funding from the Euratom Training and Research Program 2019 - 2020 under grant agreement No. 900012. The project is related to the assessment of the stability of safety-critical concrete infrastructure in connection with the problem of the lifetime extension of nuclear power plants.

REFERENCES

1. K. Field, I. Remec, Y. Le Pape. Radiation effects in concrete for nuclear power plants – Part I: Quantification of radiation exposure and radiation effects. Nuclear Engineering and Design 282 (2015) 126.
2. I. Remec et al. Characterization of Radiation Fields for Assessing Concrete Degradation in Biological Shields of NPPs. EPJ Web of Conferences 153 (2017) 05009.
3. P.M. Bruck et al. Structural assessment of radiation damage in light water power reactor concrete biological shield walls. Nuclear Engineering and Design 350 (2019) 9.
4. J. Leppänen et al. The Serpent Monte Carlo code: Status, development and applications in 2013. Annals of Nuclear Energy 82 (2015) 142.
5. O. Trofymenko et al. Serpent 2 Code Validation to Determine the VVER-1000 Nuclear Fuel Neutron Multiplication Factor within Group Constant Generation for NPP In-Core Monitoring Systems. Nuclear and Radiation Safety 2(94) (2022) 53. (Ukr)
6. V.I. Gulik et al. The Development of a Three-Dimensional Model of WWER-1000 Core Using the Monte Carlo Serpent Code for Neutron-Physical Modeling. Problems of Atomic Science and Technology 5(123) (2019) 58.
7. D. Sprinzl, V. Krýsl, P. Mikoláš. "Full-Core" VVER-1000 calculation benchmark. In: The 26th Symposium of AER on VVER Reactor Physics and Reactor Safety (Helsinki, Finland, 2016).
8. J. Leppänen et al. Development of a coupled neutron/photon transport mode in the Serpent 2 Monte Carlo Code. In: International Conference on Mathematics & Computational Methods Applied to Nuclear Science & Engineering (M&C 2017) Jeju, Korea, April 16 - 20, 2017.
9. J. Leppänen, T. Viitanen, O. Hyvöneny. Development of a Variance Reduction Scheme in the Serpent 2 Monte Carlo Code. International Conference on Mathematics & Computational Methods Applied to Nuclear Science & Engineering (M&C 2017) Jeju, Korea, April 16 - 20, 2017.
10. R. Tuominen, V. Valtavirta, J. Leppänen. New energy deposition treatment in the Serpent 2 Monte Carlo transport code. Annals of Nuclear Energy 129 (2019) 224.
11. O. Khotiaintseva et al. Photon Transport Simulation by Serpent Code: Example of Biological Shielding Calculation. Nuclear and Radiation Safety 4(92) (2021) 40. (Ukr)
12. A.M. Berezovets et al. Neutron space distribution in WWER ionization chamber channels. Problems of Atomic Science and Technology 8 (1987) 74.

О. М. Хотяїнцева[1,*], О. Р. Трофименко[1,2], В. М. Хотяїнцев[3], А. В. Носовський[1,2], С. Е. Шоломіцький[2], В. І. Гулік[1,2]

[1] Інститут проблем безпеки атомних електростанцій НАН України, Київ, Україна
[2] Товариство з обмеженою відповідальністю ЕНЕРГОРИСК, Київ, Україна
[3] Київський національний університет імені Тараса Шевченка, Київ, Україна

*Відповідальний автор: olenakhot@gmail.com

РОЗРАХУНОК РАДІАЦІЙНИХ ПОЛІВ У БЕТОНІ БІОЛОГІЧНОГО ЗАХИСТУ ВВЕР-1000 ЗА ДОПОМОГОЮ МОНТЕ-КАРЛО КОДУ SERPENT

Для розрахунку радіаційних полів у бетоні біологічного захисту ВВЕР-1000, ми розробили і застосовуємо у цій роботі методику моделювання з використанням техніки зменшення дисперсії на основі Монте-Карло коду Serpent. Розраховано радіальні, аксіальні та азимутальні залежності потоків нейтронів і гамма-променів та потужності поглинутої дози у бетоні біологічного захисту. На основі результатів розрахунків оцінено максимальні флюенси нейтронів з різними відсічками по енергії і максимальну поглинуту дозу в біологічному захисті ВВЕР-1000 за 60 і 80 років експлуатації реактора, та визначено області з найбільшим радіаційним навантаженням. Отримані результати добре узгоджуються з наявними у літературі даними щодо ВВЕР-1000 та інших реакторів типу PWR. Показано, що флюенс нейтронів з енергією вище 0,1 МеВ зменшується вдвічі на глибині 4 см бетону, а поглинута доза гамма-випромінювання зменшується на 40 % на глибині 13,5 см. Результати цього дослідження допоможуть оцінити наслідки тривалого опромінення бетону біологічного захисту ВВЕР-1000, що необхідно для достовірної оцінки ризиків, пов’язаних із продовженням термінів експлуатації атомних електростанцій.

Ключові слова: бетон біологічного захисту, опромінений бетон, Монте-Карло код Serpent, ВВЕР-1000.

Надійшла/Received 31.12.2022